

Detection of Neuroendocrine Tumors: ^{99m}Tc -P829 Scintigraphy Compared with ^{111}In -Pentetreotide Scintigraphy

Rachida Lebtahi, MD, PhD¹; Joseph Le Cloirec, MD²; Claire Houzard, MD³; Doumit Daou, MD¹; Iradj Sobhani, MD, PhD⁴; Geneviève Sassolas, MD³; Michel Mignon, MD, PhD⁴; Patrick Bourguet, MD, PhD²; and Dominique Le Guludec MD, PhD¹

¹Nuclear Medicine Department, Hôpital Bichat, Assistance Publique-Hôpitaux de Paris, Paris, France; ²Nuclear Medicine Department, Centre Eugène Marquis, Rennes, France; ³Nuclear Medicine Department, Hôpital Universitaire Neuro-Cardiologique, Lyon, France; and ⁴Gastroenterology Department, Hôpital Bichat, Assistance Publique-Hôpitaux de Paris, Paris, France

The aim of this study was to evaluate the diagnostic value of a new somatostatin analog, ^{99m}Tc -P829, compared with that of ^{111}In -pentetreotide. **Methods:** Forty-three patients (32 men, 11 women; age range, 24–78 y; mean age, 56 y) with biologically or histologically proven neuroendocrine tumors were prospectively included: 11 patients with Zollinger-Ellison syndrome, 16 patients with carcinoid tumors, and 16 patients with other types of functioning ($n = 6$) or nonfunctioning ($n = 10$) endocrine tumors. ^{111}In -Pentetreotide planar images (head, chest, abdomen, and pelvis) were obtained 4 and 24 h after injection of 10 μg somatostatin analog labeled with 148 ± 17 MBq ^{111}In , and SPECT was performed 24 h after injection. Similar ^{99m}Tc -P829 planar images were obtained at 1, 4–6, and 24 h after injection of 50 μg peptide labeled with 991.6 ± 187.59 MBq ^{99m}Tc . Abdominal SPECT was performed 4–6 h after injection. **Results:** ^{111}In -Pentetreotide detected 203 tumoral sites in 39 (91%) of 43 patients, whereas ^{99m}Tc -P829 detected 77 sites in 28 (65%) of 43 patients ($P < 0.005$). In the liver, 129 sites (in 24 patients) were detected by ^{111}In -pentetreotide scintigraphy and 34 sites (in 10 patients) were detected by ^{99m}Tc -P829 scintigraphy. **Conclusion:** In patients with endocrine tumors, the detection rate of ^{99m}Tc -P829 scintigraphy was lower than that of ^{111}In -pentetreotide scintigraphy, which appeared to be more sensitive, especially for liver metastases.

Key Words: somatostatin receptor scintigraphy; ^{99m}Tc -P829 scintigraphy; endocrine tumors

J Nucl Med 2002; 43:889–895

Most endocrine tumors express cell-surface somatostatin receptors (1–8). Scintigraphic detection of specific cellular expression is available using an indium-labeled somatostatin analog receptor tracer with a high affinity for binding to a receptor or cell product (9–16). Pentetreotide is

an analog of octreotide produced by the synthetic addition of diethylenetriaminepentaacetic acid, which provides 4 COOH groups for the formation of metal-binding complexes. ^{111}In -Pentetreotide (OctreoScan; Mallinckrodt, Inc., St. Louis, MO) is commercially available for imaging. ^{111}In -Somatostatin receptor scintigraphy is a sensitive method for the detection of endocrine tumors and their metastases (17–24). However, the potential clinical advantage of technetium labeling, compared with indium labeling, is related to lower cost, better availability, and faster tumoral visualization (1-d-protocol imaging). In addition, the physical characteristics of technetium are more adapted to the energy detection ability of gamma cameras, with a shorter physical period leading to a higher-dose administration of radiolabeled peptide and better image quality with lower radiation doses. Therefore, the technetium-labeled somatostatin analog (^{99m}Tc -P829) was developed (25). P829 is a peptide that contains a bioamino-acid-active sequence mimetic of native somatostatin. ^{99m}Tc -P829 was considered to have a biodistribution and receptor binding affinity similar to those of ^{111}In -pentetreotide (26,27). P829 peptide has the molecular formula $\text{C}_{65}\text{H}_{95}\text{N}_{16}\text{O}_{12}\text{S}_2$ and the structure R-Tyr-(D-Trp)-Lys-Val-R'-(β -Dap)-Lys-Cys-Lys-amide.

The purpose of this study was to prospectively evaluate the ability of scintigraphy using the somatostatin analog labeled with ^{99m}Tc (^{99m}Tc -P829), compared with ^{111}In -pentetreotide scintigraphy, to detect and localize endocrine tumors. The results of ^{99m}Tc -P829 and ^{111}In -pentetreotide scintigraphy were compared, with the latter considered the gold standard scintigraphic imaging procedure for the detection of endocrine tumors and their metastases. This study was part of a multicenter trial comprising 3 French centers (at Lyon, Rennes, and Paris).

MATERIALS AND METHODS

Patients

Forty-three patients (32 men, 11 women; age range, 24–78 y; mean age, 56 ± 8 y) with proven endocrine tumors were prospec-

Received Jul. 12, 2001; revision accepted Mar. 25, 2002.

For correspondence or reprints contact: Rachida Lebtahi, MD, PhD, Service de Médecine Nucléaire, Hôpital Bichat, 46 rue Henri Huchard, 75018, Paris, France.

E-mail: rachida.lebtahi@bch.ap-hop-paris.fr

tively included at 3 French centers. Written consent was obtained from all patients. The study population included 2 patients with a growth hormone-producing pituitary adenoma, 1 patient with Cushing's syndrome and with a suspected adrenocorticotrophic hormone (ACTH)-secreting tumor, and 40 patients with gastroenteropancreatic (GEP) tumors. The final diagnosis of growth hormone-producing pituitary adenoma was obtained by surgery after scintigraphy. In the patient with Cushing's syndrome and with a suspected ACTH-secreting tumor, no evidence of tumor was found by conventional imaging.

Among the 40 patients with GEP tumors, 30 patients had functioning tumors: 11 patients with Zollinger-Ellison syndrome, based on evidence of the specific biologic syndrome ($n = 11$) or histopathology findings ($n = 9$); 16 patients with a histologically confirmed carcinoid tumor; 2 patients with a glucagonoma, and 1 patient with an insulinoma. Ten patients had endocrine tumors that were proven histologically but were classified as nonfunctioning because the patients lacked any specific clinical symptoms related to hormone overproduction markers (e.g., insulin, gastrin with secretin, vasoactive intestinal peptide, glucagon, somatostatin, or serotonin).

Final diagnoses in patients considered to have a GEP tumor or metastases were based on the results of radiology (CT, MRI, arteriography, or endoscopic sonography) or of surgery and histology. In patients with multiple metastases, confirmation of metastatic involvement was not always available for all sites but was available for at least 1 tumoral site. According to radiologic findings or histology, 24 patients had known liver metastases and 4 patients had bone metastases. During the follow-up after scintigraphy, 8 patients underwent surgery (2 patients with pituitary adenomas and 6 patients with GEP tumors). Altogether, histologic confirmation of tumor was obtained (before or after scintigraphy) for 41 of 43 patients. Of the 2 patients without histologic confirmation, 1 had specific biologic evidence of Zollinger-Ellison syndrome but no evidence of tumor and 1 had Cushing's syndrome with suspicion of, but no evidence of, an ACTH-secreting tumor.

^{111}In -Pentetreotide and $^{99\text{m}}\text{Tc}$ -P829 scintigraphy were performed on each patient within 3 wk of each other.

^{111}In -Pentetreotide Imaging

A mean dose of 148 ± 17 MBq ^{111}In -pentetreotide (Mallinckrodt Medical, Petten, The Netherlands) containing $10 \mu\text{g}$ somatostatin analog was administered immediately after the specific radiochemical purity had been checked by chromatography (mean purity, $96.90\% \pm 1.85\%$).

Scintigraphic planar images were acquired using a double-head camera (DST or DST XL; SMV, Brie, France) with a medium-resolution parallel-hole collimator, a 256×256 word matrix, and a preset time of 10–15 min. Acquisition was performed using both ^{111}In photopeaks (171 and 245 keV).

Abdominal images were obtained 4 h after injection, in the anterior and posterior views. For 12 patients, 1-h images were obtained to compare ^{111}In -pentetreotide uptake with $^{99\text{m}}\text{Tc}$ -P829 uptake. At 24 h, the acquisition systematically included anterior and posterior views of the head, chest, abdomen, and pelvis. Additional lateral and oblique views were obtained when necessary. Delayed images of the abdomen were systematically obtained in the anterior and posterior views at 30–48 h after injection. When findings were negative or doubtful, acquisition time was increased from 15 to 20 min.

Abdominal SPECT was performed 24 h after injection on 37 patients. Cerebral SPECT was performed on 2 patients. The SPECT acquisition parameters were a double-indium-peak acquisition, 64 projections over a 360° rotation, 40–60 s per step, and a 64×64 matrix. Tomographic slices were obtained using iterative reconstruction (2 iterations, 8 subsets) with Hanning postfilter reconstruction.

$^{99\text{m}}\text{Tc}$ -P829 Imaging

Vials of somatostatin analog containing $50 \mu\text{g}$ P829 (Diatide, Londonderry, NH) were labeled with $1,061.9 \pm 138.1$ MBq $^{99\text{m}}\text{Tc}$ in a volume of 1 mL. The $^{99\text{m}}\text{Tc}$ -P829 was visually inspected for clarity and particles, and radiochemical purity (labeling yield) was then tested using instant thin-layer chromatography. The mean radiochemical purity was $95.06\% \pm 2.57\%$.

Safety was assessed by following up clinical signs and symptoms, with monitoring of vital signs and adverse events after intravenous administration of $^{99\text{m}}\text{Tc}$ -P829.

Scintigraphic planar images were acquired after injection of 991.60 ± 187.59 MBq $^{99\text{m}}\text{Tc}$ -P829, using the same double-head camera with a high-resolution parallel-hole collimator, a 256×256 word matrix, and a preset time of at least 10 min. Acquisition was performed using a 140-keV technetium photopeak (with a 20% window). Anterior and posterior views of the head, chest, upper abdomen, and lower abdomen were obtained at 1, 4–6, and 24 h after injection.

Abdominal SPECT was performed on the same 37 patients at 4–6 h after injection. Cerebral SPECT was performed on the same 2 patients. The SPECT acquisition parameters were a 140-keV $^{99\text{m}}\text{Tc}$ peak acquisition, 64 projections over a 360° rotation, 40–60 s per step, and a 64×64 matrix. Tomographic slices were obtained using iterative reconstruction (2 iterations, 8 subsets) with Hanning postfilter reconstruction.

Image Analysis

Scintigraphic images were visually analyzed, separately and independently for each scintigraphic method, by 2 independent observers who were unaware of the clinical presentation. A consensus reading was obtained in cases of interobserver disagreement. Images were evaluated for the presence or absence of abnormal uptake in each of the areas, for a total of 6 anatomic regions: head and neck, chest, upper abdomen (excluding the liver), liver, lower abdomen, and bone. For both scans, especially of the liver, if fewer than 10 hot spots were found, the sites were counted. If more than 10 hot spots sites were found, especially in the liver, metastases were considered multiple and counted as 10 lesions.

Quantitative analysis was used to compare ^{111}In -pentetreotide with $^{99\text{m}}\text{Tc}$ -P829 for uptake and image quality. For the comparison of physiologic tracer accumulation, scintigraphic images were acquired with both tracers at 1, 4, and 24 h after injection ($n = 12$). Lung-to-background (muscle) uptake ratios and liver-to-background (muscle) ratios were determined at 1, 4, and 24 h for ^{111}In -pentetreotide images and $^{99\text{m}}\text{Tc}$ -P829 images using the same regions of interest over lung, liver, and muscle for the 2 tracers. Also, tumor-to-background uptake ratios were determined both for 24-h ^{111}In -pentetreotide images and for 4-h (and 1-h, when obtained) $^{99\text{m}}\text{Tc}$ -P829 images using regions of interest over the lesions and the surrounding homolateral normal-uptake side. The mean counts over the lesions and background in the same regions

were calculated for ^{111}In -pentetreotide and $^{99\text{m}}\text{Tc}$ -P829 scintigraphic images.

Statistical Analysis

The McNemar test was used to compare tumoral site detection by the 2 techniques, and the paired *t* test was used to compare uptake ratios ($P < 0.05$ was considered statistically significant).

RESULTS

No adverse reactions were observed in any patients.

Tracer Accumulation

With ^{111}In -pentetreotide scintigraphy, physiologic uptake was seen in the pituitary, thyroid gland, liver, spleen, and kidneys. Bladder activity and bowel contamination were seen. With $^{99\text{m}}\text{Tc}$ -P829 scintigraphy, physiologic uptake was seen in the pituitary, thyroid gland, lung, bone marrow, liver, spleen, and kidneys. Bladder activity and bowel contamination were seen and appeared more marked than on ^{111}In -pentetreotide images.

Compared with ^{111}In -pentetreotide scintigraphy, $^{99\text{m}}\text{Tc}$ -P829 scintigraphy showed a higher nonspecific uptake in the thorax (lung and bone marrow) (at 4 h, 3.54 ± 2.2 vs. 4.44 ± 1.83 , $P < 0.0004$; at 24 h, 3.21 ± 0.56 vs. 3.75 ± 0.82 , $P < 0.03$). In the liver, uptake was also higher with $^{99\text{m}}\text{Tc}$ -P829 scintigraphy at 4 h and was similar at 24 h (at 4 h, 7.82 ± 2.31 vs. 3.49 ± 0.66 , $P < 0.0006$; at 24 h, 8.7 ± 2.45 vs. 7.3 ± 2.12 , not statistically significant).

Tumoral Site Detection

The results are summarized in Table 1. ^{111}In -Pentetreotide scintigraphy showed abnormal findings in 39 (91%) of 43 patients and detected 203 tumoral sites. $^{99\text{m}}\text{Tc}$ -P829 scintigraphy showed abnormal findings in 28 (65%) of 43 patients and detected 77 tumoral sites ($P < 0.005$) (Figs. 1 and 2).

Focusing on liver metastases, 129 sites (24 patients) were detected by ^{111}In -pentetreotide scintigraphy and 34 sites (10 patients) were detected by $^{99\text{m}}\text{Tc}$ -P829 scintigraphy (Figs. 3 and 4). All liver metastases detected with $^{99\text{m}}\text{Tc}$ -P829 scintigraphy were also and better visualized with ^{111}In -pentetreotide scintigraphy.

One hundred nine tumoral sites were detected only by ^{111}In -pentetreotide scintigraphy, whereas 3 tumoral sites (1

orbital and 2 lung and mediastinum) were detected only by $^{99\text{m}}\text{Tc}$ -P829 scintigraphy.

Among the 4 patients who had no abnormalities detected by ^{111}In -pentetreotide, 1 patient had an elevated serotonin level and a liver metastasis detected by abdominal CT and confirmed by surgery after somatostatin receptor scintigraphy (carcinoid tumor); 1 patient had biologic Zollinger-Ellison syndrome and negative conventional imaging findings; 1 patient had Cushing's syndrome, suspicion of ACTH-secreting tumor, and negative conventional imaging findings; and 1 patient underwent scintigraphy as a follow-up to previous surgery for resection of primary pancreatic tumor and also had negative conventional imaging and biologic findings.

Image Quality

The ratio of tumoral uptake to normal-tissue uptake was significantly higher for ^{111}In -pentetreotide scintigraphy than for $^{99\text{m}}\text{Tc}$ -P829 scintigraphy (at 4 h, 5.82 ± 5.99 vs. 3.38 ± 3.97 , $P = 0.008$; at 24 h, 5.03 ± 6.00 vs. 2.27 ± 2.55 , $P = 0.03$). Focusing on liver tumors, the ratio of tumoral uptake to normal-tissue uptake was significantly higher for ^{111}In -pentetreotide scintigraphy than for $^{99\text{m}}\text{Tc}$ -P829 scintigraphy (at 4 h, 6.69 ± 6.71 vs. 3.56 ± 4.81 , $P = 0.02$; at 24 h, 7.45 ± 8.36 vs. 2.34 ± 3.38 , $P = 0.04$).

DISCUSSION

Somatostatin receptors have been found in a variety of endocrine and nonendocrine tumors, with 5 subtypes of receptors individualized (1–7,15). The specific role of each subtype is not clear. ^{111}In -Pentetreotide, a synthetic analog of somatostatin successfully used for staging and therapeutic management in patients with endocrine tumors, is highly sensitive for tumoral detection (28–33). Uptake of ^{111}In -pentetreotide has been shown to be related to receptor subtypes 2 and 5 (6–9). However, the expense of producing ^{111}In on a cyclotron, the limitation placed on the dose size by the long half-life of ^{111}In , and the need to wait 24–48 h after injection for optimum detection of tumors have led to a search for a technetium-labeled somatostatin analog. $^{99\text{m}}\text{Tc}$ -P829 is a synthetic somatostatin analog, that is, a peptide containing a bioactive amino acid sequence mimetic to native somatostatin. This radiopharmaceutical is safe, having no adverse clinical events and clearing rapidly from the blood after intravenous injection (25–27,34). Uptake of $^{99\text{m}}\text{Tc}$ -P829 has been found to be related to receptor subtypes 2 and 5, similar to in vitro uptake of ^{111}In -pentetreotide (26).

In our study, which was a part of a multicenter trial, the results of ^{111}In -pentetreotide scintigraphy were compared with the results of $^{99\text{m}}\text{Tc}$ -P829 scintigraphy for 43 patients with proven endocrine tumors. Compared with ^{111}In -pentetreotide scintigraphy, $^{99\text{m}}\text{Tc}$ -P829 scintigraphy showed a significantly higher nonspecific uptake in the lungs and bone marrow. In the liver, uptake was also significantly

TABLE 1
Number of Tumor Sites Revealed by
 ^{111}In -Pentetreotide and $^{99\text{m}}\text{Tc}$ -P829

Tumor site	^{111}In -Pentetreotide	$^{99\text{m}}\text{Tc}$ -P829
Head and neck	6	5
Lung and mediastinum	10	11
Liver	129	34
Celiac area: upper abdomen	41	23
Lower abdomen	7	2
Bone	10	2
Total	203	77

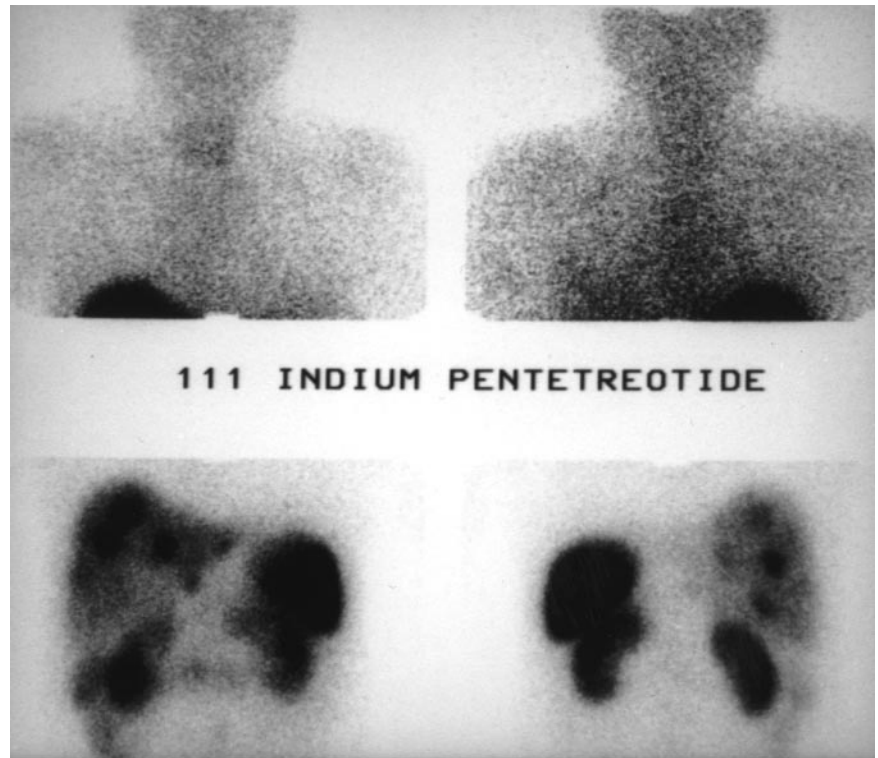


FIGURE 1. Patient with nonfunctioning endocrine tumor. ^{111}In -pentetreotide scintigraphy shows celiac tumors with liver metastases.

higher with $^{99\text{m}}\text{Tc}$ -P829 scintigraphy. In addition, ^{111}In -pentetreotide scintigraphy detected tumoral sites in 91% of patients, whereas $^{99\text{m}}\text{Tc}$ -P829 scintigraphy detected tumoral sites in 65%. Despite the higher octreotide dose used for the

$^{99\text{m}}\text{Tc}$ -P829 (50 μg) than for ^{111}In -pentetreotide (10 μg), lesion contrast was higher for ^{111}In -pentetreotide than for $^{99\text{m}}\text{Tc}$ -P829, as reflected by the tumoral uptake ratio. The significant difference found between the tracers suggests

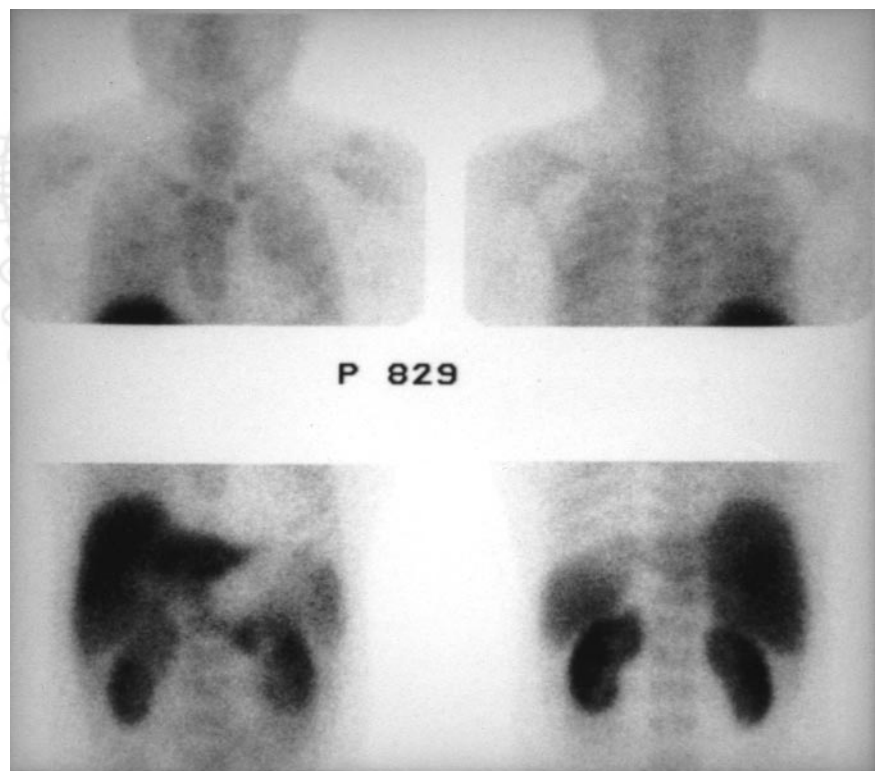


FIGURE 2. Same patient as in Figure 1. Celiac tumoral and liver metastases are not shown by $^{99\text{m}}\text{Tc}$ -P829 scintigraphy.

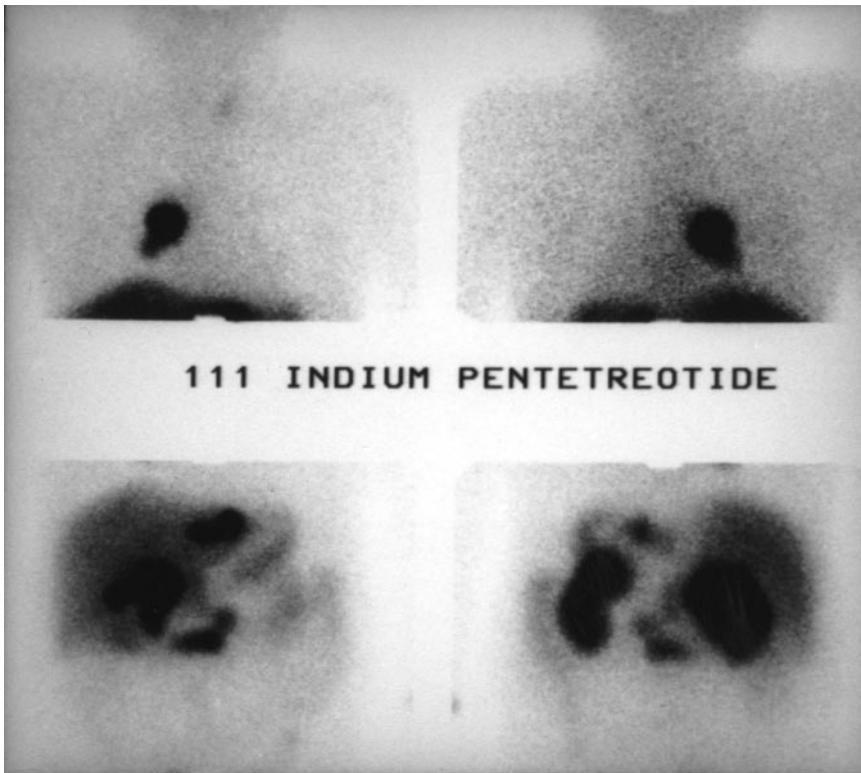


FIGURE 3. Patient with Zollinger-Ellison syndrome. ^{111}In -pentetreotide scintigraphy shows multiple celiac tumors with liver and lung metastases.

that, compared with ^{111}In -pentetreotide, $^{99\text{m}}\text{Tc}$ -P829 is less adapted to the detection of endocrine tumors.

These findings are probably related to a different in vivo biodistribution for the 2 tracers and, in part, explain the

lower tumoral uptake ratio with $^{99\text{m}}\text{Tc}$ -P829. Another explanation may be that the in vivo receptor binding affinity of $^{99\text{m}}\text{Tc}$ -P829 is different from that of ^{111}In -pentetreotide.

The lower sensitivity of $^{99\text{m}}\text{Tc}$ -P829 scintigraphy cannot

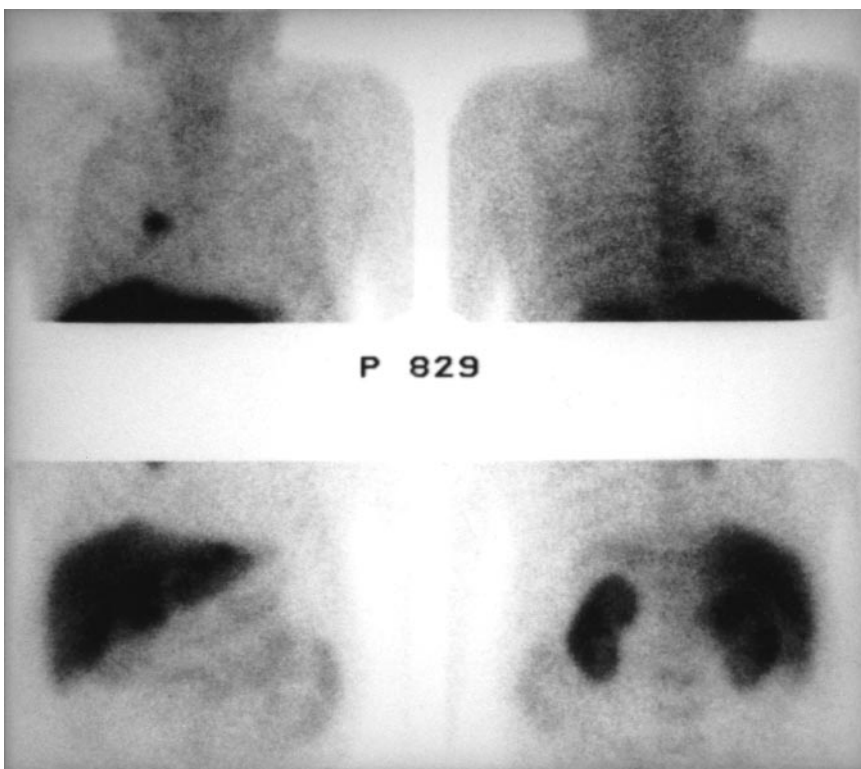


FIGURE 4. Same patient as in Figure 3. $^{99\text{m}}\text{Tc}$ -P829 scintigraphy shows lung metastases (smaller than those shown by ^{111}In -pentetreotide scintigraphy). Celiac tumors are not detected. Liver metastases are not clearly seen.

be related to the labeling procedure. Forty-five patients at 3 different French centers were included in this series; the labeling instructions were carefully followed in all cases, and the radiochemical purity was always found to be at least 90%. However, for lung cancer, Blum et al. (34) reported ^{99m}Tc -P829 scintigraphy to have a high sensitivity and a high specificity (respectively, 93% and 88%) in the detection of non-small cell cancer in patients with solitary pulmonary nodules. Malignancy in radiologically indeterminate solitary pulmonary nodules was correctly identified or excluded. The sensitivity and specificity compared favorably with the reported results for ^{18}F -FDG PET imaging. In this study, a comparison with ^{111}In -pentetreotide was not performed. However, in comparison with previously reported results for ^{111}In -pentetreotide in non-small cell cancer (35), these results suggest that ^{99m}Tc -P829 is superior and has better imaging characteristics. In this study, both biopsy material and large sections from non-small cell tumors were somatostatin receptor negative. Our results for patients with nonendocrine lung cancer who were included in the multicenter trial reported by Blum et al. were similar and showed a high uptake in lung tumors and metastases.

Another study, of patients with endocrine tumors, found better results for a ^{99m}Tc -somatostatin analog using ^{99m}Tc -tricine-HYNIC-Tyr³-octreotide than for ^{111}In -pentetreotide (36). However, whole-body clearance and absolute tumoral targeting of this compound need to be optimized, and instead of using tricine as coligand, the investigators used ethylene diamine diacetic acid (37), which has been found to result in complexes with higher stability, lower lipophilicity, lower protein binding, and higher tumor-to-organ ratios (38). The first clinical results reported showed better imaging properties than for ^{111}In -labeled derivatives (39).

CONCLUSION

In a comparison with ^{99m}Tc -P829 scintigraphy for detection of endocrine tumors, ^{111}In -pentetreotide clearly remained the most sensitive tracer. The reason for this difference in performance is unclear, considering the similar in vitro biodistributions of the tracers, but may possibly be related to a difference in somatostatin receptor binding affinity in vivo or to a difference in somatostatin receptor binding subtypes.

REFERENCES

1. Reubi JC, Häcki WH, Lamberts SWJ. Hormones producing gastrointestinal tumors contain a high density of somatostatin receptors. *J Clin Endocrinol Metab.* 1987;65:1127–1134.
2. Reubi JC, Kvols L, Krenning EP, Lamberts SWJ. Distribution of somatostatin receptor in normal and tumour tissue. *Metabolism.* 1990;30(suppl 2):78–81.
3. Reubi JC, Kvols L, Krenning E, Lamberts SW. In vivo and in vitro detection of somatostatin receptors in human malignant tissues. *Acta Oncol.* 1991;30:463–468.
4. Reubi JC, Krenning E, Lamberts SW, Kvols L. In vitro detection of somatostatin receptors in human tumors. *Digestion.* 1993;54:76–83.
5. John M, Meyerhof W, Richter D, et al. Positive somatostatin receptor scintigra-

phy correlates with the presence of somatostatin receptor subtype 2. *Gut.* 1996;38:33–39.

6. Reubi JC, Schaefer JC, Markwalder R, Waser B, Horisberger U, Laissue J. Distribution of somatostatin receptors in normal and neoplastic human tissues: recent advances and potential relevance. *Yale J Biol Med.* 1997;70:471–479.
7. Hofland LJ, Liu Q, Van Koetsveld PM, et al. Immunohistochemical detection of somatostatin receptor subtypes sst1 and sst2A in human somatostatin receptor positive tumors. *J Clin Endocrinol Metab.* 1999;84:775–780.
8. Reubi JC, Schar JC, Waser B, et al. Affinity profiles for human somatostatin receptor subtypes SST1–SST5 of somatostatin radiotracers selected for scintigraphic and radiotherapeutic use. *Eur J Nucl Med.* 2000;27:273–282.
9. Lamberts SWJ, Bakker WH, Reubi JC, Krenning EP. Somatostatin receptor imaging in the localization of endocrine tumors. *N Engl J Med.* 1990;323:1246–1249.
10. Lambert SWJ, Hofland LJ, Van Koetsveld PM, et al. Parallel in vivo and in vitro detection of functional somatostatin receptors in human endocrine pancreatic tumors: consequences with regard to diagnosis, localization, and therapy. *J Clin Endocrinol Metab.* 1990;71:566–574.
11. Lamberts SWJ, Krenning EP, Reubi JC. The role of somatostatin and its analogs in the diagnosis and treatment of tumors. *Endocr Rev.* 1991;12:450–482.
12. Lamberts SWJ, Chayvialle J-A, Krenning EP. The visualization of gastroenteropancreatic tumors. *Metabolism.* 1992;9:111–115.
13. Pauwels S, Leners N, Fiasse R, et al. Localization of gastroenteropancreatic tumors with ^{111}In pentetreotide scintigraphy. *Semin Oncol.* 1994;21:15–20.
14. Krenning EP, Kwekkeboom DJ, Bakker WH, et al. Somatostatin receptor scintigraphy with [^{111}In -DTPA-D-Phe1]- and [^{123}I -Tyr3]-octreotide: the Rotterdam experience with more than 1000 patients. *Eur J Nucl Med.* 1993;20:716–731.
15. Kwekkeboom DJ, Krenning EP, Bakker WH, et al. Somatostatin receptor scintigraphy in carcinoid tumours. *Eur J Nucl Med.* 1993;20:283–292.
16. Leners N, Jamar F, Fiasse R, Ferrant A, Pauwels S. Indium-111-pentetreotide uptake in endocrine tumors and lymphoma. *J Nucl Med.* 1996;37:916–922.
17. Alexander HR, Fraker DL, Norton JA, et al. Prospective study of somatostatin receptor scintigraphy and its effect on operative outcome in patients with Zollinger-Ellison syndrome. *Ann Surg.* 1998;228:228–238.
18. De Kerviler E, Cadiot G, Lebtahi R, Faraggi M, Le Guludec D, Mignon M. Somatostatin receptor scintigraphy in forty-eight patients with the Zollinger-Ellison syndrome. *Eur J Nucl Med.* 1994;21:1191–1197.
19. Zimmer T, Ziegler K, Bader M, et al. Localisation of neuroendocrine tumours of the upper gastrointestinal tract. *Gut.* 1994;35:471–475.
20. Scherubl H, Bader M, Fett U, et al. Somatostatin-receptor imaging of neuroendocrine gastroenteropancreatic tumors. *Gastroenterology.* 1993;105:1705–1709.
21. Kvols LK. Medical oncology considerations in patients with metastatic neuroendocrine carcinomas. *Semin Oncol.* 1994;21:56–60.
22. Yim JH, Siegel BA, De Benedetti MK, Norton JA, Lairmore TC, Doherty GM. Prospective study of the utility of somatostatin-receptor scintigraphy in the evaluation of patients with multiple endocrine neoplasia type 1. *Surgery.* 1998;124:1037–1042.
23. Gibril F, Reynolds JC, Chen CC, et al. Specificity of somatostatin receptor scintigraphy: a prospective study and effects of false-positive localizations on management in patients with gastrinomas. *J Nucl Med.* 1999;40:539–553.
24. Vallabhajosula S, Moyer BR, Lister-James J, et al. Preclinical evaluation of technetium-99m-labeled somatostatin receptor-binding peptides. *J Nucl Med.* 1996;37:1016–1022.
25. Lister-James J, Moyer BR, Dean T. Small peptides radiolabeled with ^{99m}Tc . *Q J Nucl Med.* 1996;40:221–233.
26. Virgolini I, Leimer M, Handmaker H, et al. Somatostatin receptor subtype specificity and in vivo binding of a novel tumor tracer, ^{99m}Tc -P829. *Cancer Res.* 1998;58:1850–1859.
27. Jamar F, Fiasse R, Leners N, Pauwels S. Somatostatin receptor imaging with indium-111-pentetreotide in gastroenteropancreatic neuroendocrine tumors: safety, efficacy and impact on patient management. *J Nucl Med.* 1995;36:542–549.
28. Anthony LB, Martin W, Delbeke D, Sandler M. Somatostatin receptor imaging: predictive and prognostic considerations. *Digestion.* 1996;57:50–53.
29. Termanini B, Gibril F, Reynolds JC, et al. Value of somatostatin receptor scintigraphy: a prospective study in gastrinoma of its effect on clinical management. *Gastroenterology.* 1997;112:335–347.
30. Lebtahi R, Cadiot G, Sarda L, et al. Clinical impact of somatostatin receptor scintigraphy in the management of patients with neuroendocrine gastroenteropancreatic tumors. *J Nucl Med.* 1997;38:853–858.
31. Chiti A, Fanti S, Savelli G, et al. Comparison of somatostatin receptor

- imaging, computed tomography and ultrasound in the clinical management of neuroendocrine gastro-entero-pancreatic tumours. *Eur J Nucl Med.* 1998;25:1396–1403.
32. Lebtahi R, Cadiot G, Delahaye N, et al. Detection of bone metastases in patients with endocrine gastroenteropancreatic tumors: bone scintigraphy compared with somatostatin receptor scintigraphy. *J Nucl Med.* 1999;40:1602–1608.
 33. Blum JE, Handmaker H, Rinne NA. The utility of a somatostatin-type receptor binding peptide radiopharmaceutical (P829) in the evaluation of solitary pulmonary nodules. *Chest.* 1999;115:224–232.
 34. Blum J, Handmaker H, Lister-James J, Rinne N. A multicenter trial with a somatostatin analog (^{99m}Tc depreotide) in the evaluation of solitary pulmonary nodules. *Chest.* 2000;117:1232–1238.
 35. Kwekkeboom DJ, Kho GS, Lamberts SW, Reubi JC, Laissue JA, Krenning EP. The value of octreotide scintigraphy in patients with lung cancer. *Eur J Nucl Med.* 1994;21:1106–11013.
 36. Bangard M, Béhé M, Gohlke S, et al. Detection of somatostatin receptor-positive tumours using the new ^{99m}Tc -tricine-HYNIC-d-Phe1-Tyr3-octreotide: first results in patients and comparison with ^{111}In -DTPA-d-Phe1-octreotide. *Eur J Nucl Med.* 2000;26:628–637.
 37. Gohlke S, Bangard M, Buschmann I, Béhé M, Maecke HR, Biersack HJ. ^{99m}Tc -EDDA-HYNIC-Tyr3-octreotide for detection of somatostatin receptor positive tumors and first experience in patients [abstract]. *J Nucl Med.* 2000;41(suppl):149P.
 38. Decristoforo C, Melendez-Alafort L, Sosabowski JK, Mather SJ. ^{99m}Tc -HYNIC-[Tyr3]-octreotide for imaging somatostatin-receptor-positive tumors: preclinical evaluation and comparison with ^{111}In -octreotide. *J Nucl Med.* 2000;41:1114–1119.
 39. Decristoforo C, Mather SJ, Cholewinski W, Donnemiller E, Riccabona G, Moncayo R. ^{99m}Tc -EDDA/HYNIC-TOC: a new ^{99m}Tc -labelled radiopharmaceutical for imaging somatostatin receptor-positive tumours—first clinical results and intra-patient comparison with ^{111}In -labelled octreotide derivatives. *Eur J Nucl Med.* 2000;27:1318–1325.

